Catalysis Science & Technology

ROYAL SOCIETY OF CHEMISTRY

PAPER

View Article Online
View Journal

Cite this: DOI: 10.1039/d5cy01499a

Elucidating activity-property relationships of dual catalysts for poly(ethylene terephthalate) depolymerisation

Matt J. Price,[a] Anna Bachs-Herrera,[bc] Arianna Brandolese,[a] Yuya Watanabe,[a] Matthew N. Grayson,*[b] Antoine Buchard*[c] and Andrew P. Dove*[a]

Received 8th December 2025,
Accepted 6th April 2026

DOI: 10.1039/d5cy01499a

rsc.li/catalysis

Polyethylene terephthalate (PET) is one of the most prominent single-use plastics. It can be readily circularised *via* chemical depolymerisation to monomer and subsequent repolymerisation to deliver virgin quality PET from waste. Chemical recycling-to-monomer (CRM) approaches rely on catalysts to enhance the activity of the depolymerisation process. Recently, dual-catalytic systems that combine inexpensive and readily available Lewis acids with simple organobases have displayed cooperative catalytic activity, among the highest reported for these processes; however, their mechanism of action, alongside the large number of possible combinations, makes identifying ideal catalyst species challenging. In this manuscript, we systematically explore the relationship between metal Lewis acids and organobases and their impact on PET glycolysis activity. These studies reveal a relationship between metal acetate electronegativity and the pK_a of the organobase that can be used to predict the most active combination for a given metal salt or organobase. Furthermore, through preliminary DFT calculations, we demonstrate that the glycolysis likely follows a mechanism in which the base coordinates to the Lewis acid, acting as a single catalytic entity, and in which the acetate ligand assists with proton transfer.

Introduction

Plastic production has sharply increased over the last 70 years, driven by an ever-increasing demand for plastics in everyday life.[1] Unfortunately, plastic recyclability protocols have not kept up with its huge consumption and thus waste has accumulated in the environment and landfills. Poly(ethylene terephthalate) (PET) is one of the most widely used common plastics that accounts for almost 20% of global plastic demand.[2–4] Current legislative efforts are providing an environment that is conducive to recycling, which, along with stringent regulations, is leading to new opportunities for the implementation of alternative and optimised schemes for the collection, sorting, and processing of PET waste to achieve a circular plastic economy while contributing to sustainable development.[5–7]

Where PET is collected, the waste processing industry applies mechanical recycling and reprocessing methods that can result in a product that can be used for the same initial purpose. However, over time, the properties of the polymer degrade, and it becomes contaminated with dirt and other debris that impact both its performance and appearance, leading to "downcycling" into lower-value products. Chemical recycling-to-monomer (CRM) offers a valuable alternative to mechanical recycling, enabling the depolymerisation of waste PET back to monomers from which recycled polymers that possess the same properties as virgin material can be made.

To date, PET chemical recycling has been exploited through hydrosilylation,[8–10] hydrogenolysis,[11] and recently by both glycolysis[12–16] and alcoholysis[17,18] processes; the latter approaches present the most viable solutions for depolymerisation/repolymerisation cycles at scale.[12,19–26] Most focus has been directed towards PET glycolysis to bis(2-hydroxyethylene)terephthalate (BHET) using both metal-based and organic catalysts.[22,27,28] The requirement to operate at high temperatures in the presence of protic sources makes catalyst design challenging, hence simple metal salts, such as $Zn(OAc)_2$ are among the most widely studied, as well as being used in industrial PET glycolysis processes. Ionic liquids have also been widely studied and employed as recyclable catalysts, including in commercial settings, offering good depolymerisation activity and separation potential.[29–31] More recently, organic salt catalysts, made from organic acids and bases, have also

[a] School of Chemistry, University of Birmingham, Edgbaston, Birmingham, B15 2TT, UK
[b] Department of Chemistry, University of Bath, Claverton Down, Bath, BA2 7AY, UK
[c] Department of Chemistry, Green Chemistry Centre of Excellence, University of York, York, YO10 5DD, UK

been applied for PET glycolysis.[28] These salts have been almost all found to be more thermally stable than their component parts, and hence remain more highly active over longer time periods (or catalyst recycle loops) compared to the base catalysts alone.[22,32,33] Several other studies, including our own, have shown a significant rate enhancement when metal acetates (*e.g.* zinc(II), manganese(II), copper(II) and nickel(II)) are combined with organic bases (*e.g.* tropine, 4-dimethylaminopyridine, DMAP, *etc.*), with high catalyst stability.[14,22,34–36] Notably, the combination of species results in a synergistic effect where the activity of the combination is greater than the sum of the parts, proposed to be a result of a dual catalytic mechanism in which the Lewis acid and the base act as separate entities, but in tandem.

The large number of potential combinations of inexpensive, commercially available and earth-abundant metal salts and organic bases that could act as PET glycolysis catalysts presents significant potential to enhance catalyst activity in a practical manner. In turn, this could enable depolymerisation to occur in a more energy-efficient manner, for example, at a lower temperature, or to enable access to a wider range of alcoholysis reactions that might, at present, be excluded as a consequence of the high reaction temperatures applied. To this end, to advance catalyst design towards these goals, we sought to develop a fundamental understanding of the proposed dual catalytic mechanism through experimental and computational methods and hence elucidate the key features of the catalyst components that allowed for predictable selection of highly active catalytic combinations of metal salts and organic bases.

Results and discussion

Our study initially focused on the measurement of the activity of a range of dual catalysts formed from a 1:1 combination of Lewis acids and organobases for PET depolymerisation at 180 °C, with 1 mol% catalyst loading with respect to each component (Fig. 1A). As expected, lower catalyst loadings resulted in reduced activity, with 1 mol% representing the optimal compromise between catalyst loading and reaction time (Fig. S17). Initially, organobases with pK_aH ranging from 5 to 11 were screened using $Zn(OAc)_2$ as the metal salt catalyst. Depolymerisation was assessed by monitoring the appearance of BHET in solution using ^{1}H NMR spectroscopy of samples taken from the reactions, which contain *N*-methyl-2-pyrrolidone (NMP) as an internal standard. The initial rate constants, k', were derived from the conversion-time plots (Fig. S8–S11) and analysed using a 'shrinking core' model (eqn (S1)) on account of the heterogeneous nature of the depolymerisation reaction. Analysis of the initial rate constants with respect to pK_aH of the organobase revealed no clear trend, with a peak of activity appearing for the combination of $Zn(OAc)_2$ with imidazole, Im (pK_aH = 6.9), a weak base, and lowest activity when

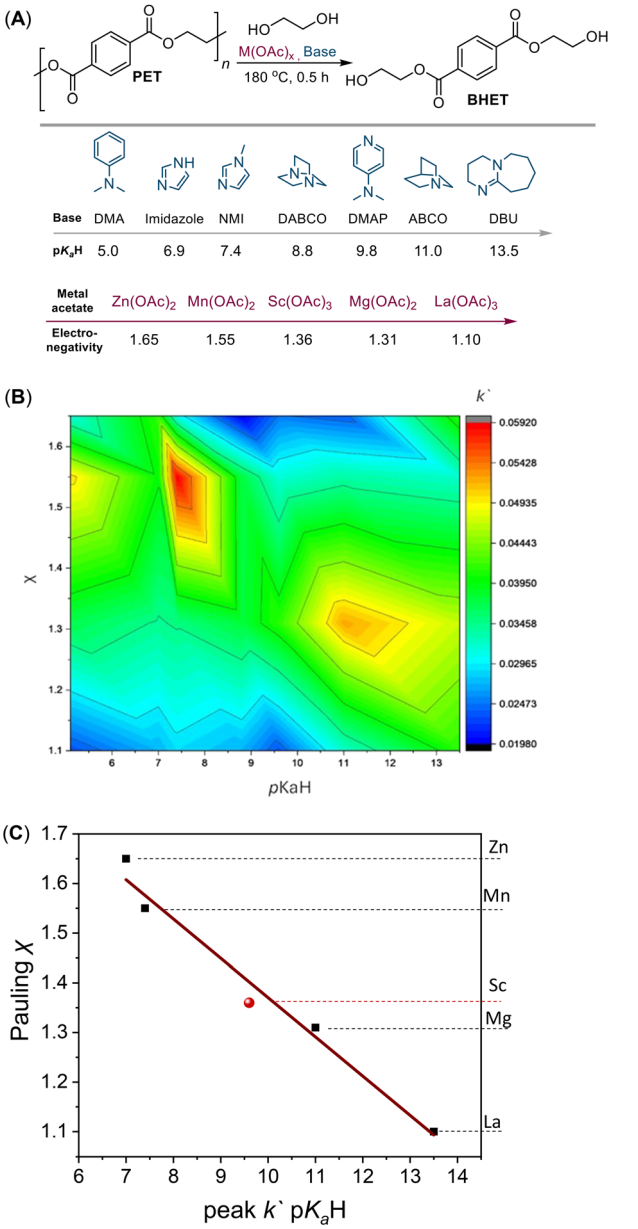

Fig. 1 (A) General reaction scheme for PET glycolysis to BHET promoted by Lewis acids and organobases, and Lewis acids and organobases explored in this work. (B) First-order rate constants (k', min^{-1}) for the metal acetate-base combinations, showing the pK_aH of the bases and the electronegativity of the metal acetates on the x and y axes, respectively. (C) pK_aH at peak activity shows an inverse relationship with metal acetate electronegativity (R^2 = 0.989).

1,4-diazabicyclo[2.2.2]octane, DABCO (pK_aH = 8.8) was used as the cocatalyst.

In search of more active catalyst combinations, we sought to develop an understanding of how the activity trend differed when the bases were combined with other metal acetates for catalysing PET glycolysis. To survey the impact of Lewis acid, three further metal acetates, $La(OAc)_3$, $Mg(OAc)_2$, $Mn(OAc)_2$, were selected on account of their wide range of electronegativity (as determined by Pauling electronegativity (χ) values) and studied for depolymerisation of PET with each

of the organic bases applied previously with $Zn(OAc)_2$. Determination of the initial depolymerisation rate for each metal salt/base combination revealed that a different base provided peak activity for each different metal salt (Fig. 1B, Fig. S8–S11). $La(OAc)_3$/base dual catalysts display a relatively clear trend of increased base pK_aH correlating to increased activity (Fig. S10), likely a consequence of base dominated activity on account of the relative weakness of $La(OAc)_3$ as a Lewis acid and poor activity as a glycolysis catalyst, with peak activity achieved with 1,8-diazabicyclo(5.4.0)undec-7-ene, DBU (pK_aH = 13.5). Similar analysis for $Mg(OAc)_2$ and $Mn(OAc)_2$ as the Lewis acid revealed peak activities with 1-azabicyclo[2.2.2] octane, ABCO (pK_aH = 11.0) and *N*-methyl imidazole, NMI (pK_aH = 7.4), respectively. An analogous correlation is observed when considering the bases pK_aHs values in MeCN and the metal acetate electronegativity (Fig. S12).

To explain the combinations that led to peak activity for all the catalyst combinations, we examined possible relationships between characteristics of the Lewis acid (Pauling electronegativity, ionic radius, Pearson hardness and Gagne–Hawthorne length) and organic base pK_aH. Interestingly, plotting the Pauling electronegativity (χ) of the metal and the pK_aH of the organic base for the combinations that displayed the highest activity for depolymerisation revealed a clear linear trend in which the metal acetate with the highest Pauling electronegativity was most active with the base with the lowest pK_aH and conversely, the metal acetate with the lowest Pauling electronegativity was most active with the base with the highest pK_aH (Fig. 1C and S12). To verify this observation, scandium acetate ($Sc(OAc)_3$) was selected as it has a Pauling electronegativity value of χ = 1.36, between that of $Mg(OAc)_2$ and $Mn(OAc)_2$. The correlation predicted that a base with pK_aH around 10 would provide the combination of peak activity, which was confirmed with depolymerisation tests using $Sc(OAc)_3$/base combinations with DABCO, DMAP and ABCO in which the peak activity was achieved with $Sc(OAc)_3$ and DMAP (base pK_aH = 9.6), which falls closest to the linear relationship between peak k', pK_aH and χ (red sphere, Fig. 1C). To elucidate the catalyst structure, additional studies were conducted to investigate the potential coordination of ethylene glycol and NMP to the metal acetate (Fig. S13–S16). $Zn(OAc)_2$ was examined in the presence of varying ratios of ethylene glycol and NMP, and the mixtures were monitored by NMR spectroscopy. Only negligible spectral shifts were observed for $Zn(OAc)_2$, indicating that ethylene glycol and NMP are unlikely to coordinate to the zinc centre under the glycolysis conditions tested. Additionally, all tested catalysts were insoluble in ethylene glycol at 180 °C (Fig. S18).

To gain a deeper insight into the role of each single catalyst component for PET glycolysis and confirm that the peak dual catalyst combinations retained the synergistic effect in which the combined activity was greater than the sum of the catalytic activity of the individual components, we screened PET depolymerisation activity of the Lewis acids and organic bases as standalone catalysts. Simply surveying PET depolymerisation activity when catalysed by the range of organic bases studies reveals a simple trend that relates initial depolymerisation rate to pK_aH, in which the activity generally increases as the pK_aH increases, in line with stronger bases being better at activating the ethylene glycol towards nucleophilic attack on the PET (Fig. S3). Screening metal acetate catalysts found that the activity was in the order of $Mn(OAc)_2 > Mg(OAc)_2 > Zn(OAc)_2 \approx La(OAc)_3$ (Table S2). While $Zn(OAc)_2$ is most commonly used as a catalyst,[37] these results agree with previously reported works, which place $Mn(OAc)_2$ as more efficient than $Zn(OAc)_2$.[38] Correlation between activity and metal acetate physical parameters was conducted through the aid of a linear regression analysis of the proxy variables with activity. Regression analysis showed an inversely proportional relationship with both electronegativity and ionic radius, implying that smaller, less electronegative metal ions have higher activity. This indicates that what defines ultimate catalyst activity may be more complicated than simply evaluation of the metal acetate electronegativity, in line with the observation that the most active dual catalyst system was $Mn(OAc)_2$/NMI. Notably, however, in each case, the combination of metal acetate and organic base displayed between 1.5 and 3× higher k' than the sum of the metal acetate and organic base k' values (Table S2 and Fig. S2–S5). This strongly indicates that the combination of metal acetate and organic base results in a more active catalyst species than could be obtained from both species acting independently.

The property-activity relationships suggest that the origins of the synergistic effect between metal acetate and organic base may be more complex than initially assumed in the dual catalyst mechanism (Fig. 2). Therefore, Density Functional Theory (DFT) calculations were undertaken using Gaussian 16, Revisions C.01 (ref. 39) and C.02 (ref. 40) to elucidate the more intricate relationships between mechanism, properties and activity. As outlined previously, we had anticipated that interactions between the metal acetate and organic base would lead to the base being bound to the metal centre at room temperature, but to unbind at the reaction temperature of 453 K where it could undertake a dual catalyst mechanism. The possibility of a complex formation between the metal acetate and base was therefore explored by DFT calculations, focusing on $Zn(OAc)_2$ as a representative system. Calculation of the binding Gibbs free energies ($\Delta G_{binding}$) of $Zn(OAc)_2$ and each of the organic bases employed experimentally revealed a reversible process with $\Delta G_{binding} \approx 0$ for bases with pK_aH between 6.9 and 11. At the extremes of pK_aH a clear thermodynamic preference for being bound or unbound was observed. Binding of DMA (pK_aH = 5.0) was unfavourable ($\Delta G_{binding}$ = +10.8 kcal mol^{-1}), whereas, in contrast, interaction with the strong base, DBU, (pK_aH = 13.5) revealed that the binding of the base to metal was thermodynamically favourable, $\Delta G_{binding}$ = −4.2 kcal mol^{-1}. $\Delta G_{binding}$ for bases with pK_aH between these extremes were closer to zero (Fig. 3). This finding suggests that base strength may

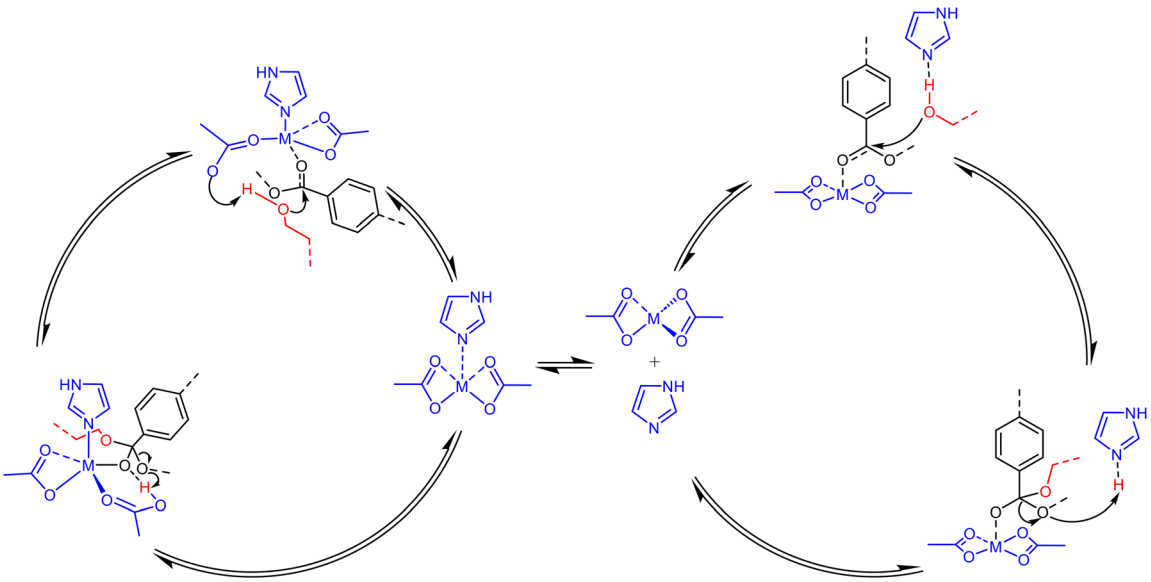

Fig. 2 Schematics of the two proposed mechanisms of PET glycolysis: bound (left) and unbound (right) pathways.

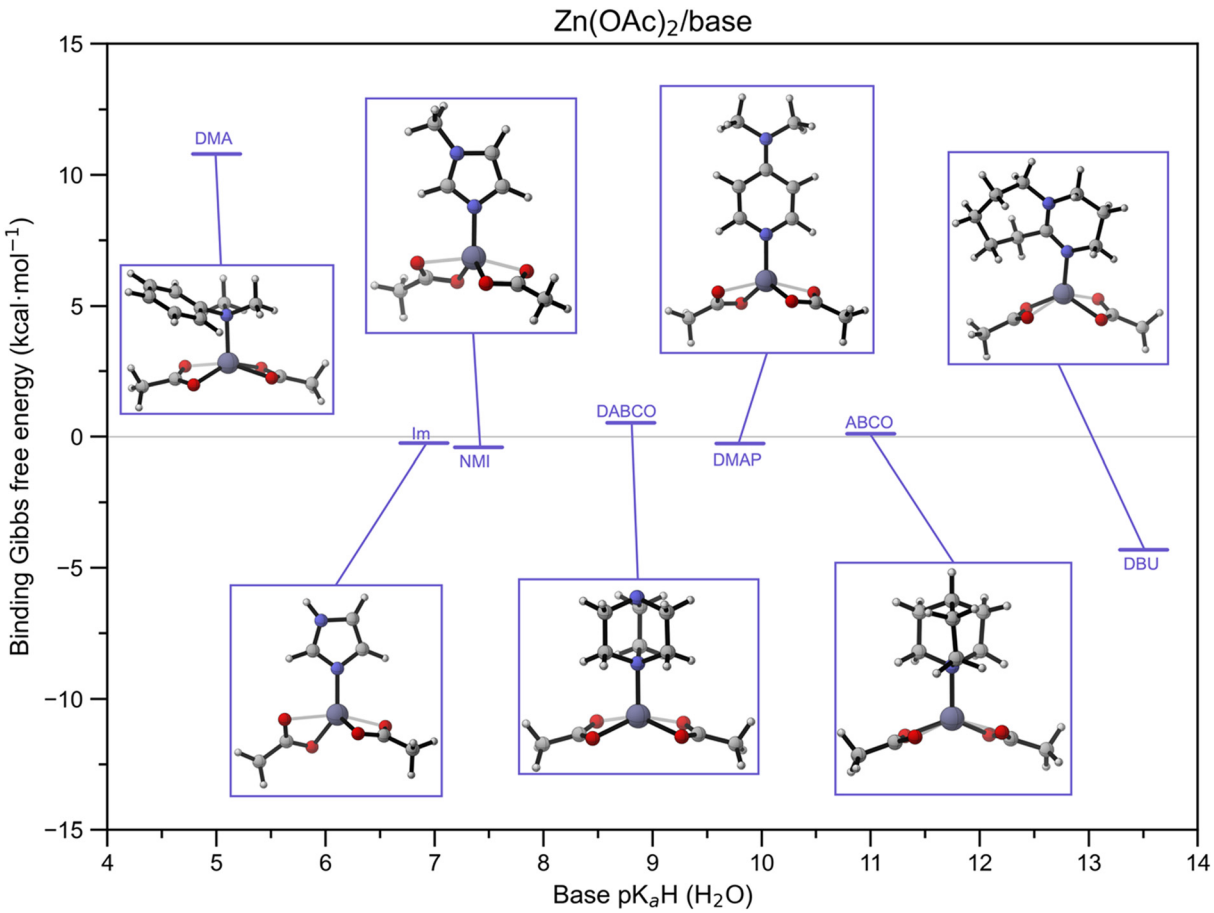

Fig. 3 $Zn(OAc)_2$/base complex geometries and binding Gibbs free energies. The systems were optimised at ωB97X-D/6-31G(d) level of theory and with single point energy calculation at the ωB97X-D/def2-TZVP level of theory, both with the CPCM implicit solvent model for 1,2-ethanediol at 453 K (ε = 19.1).[45] Images were created using CYLview 1.0 beta.[46]

influence the mechanism by which depolymerisation occurs, with stronger bases interacting more strongly with Zn^{2+}, although steric factors may also play an important role in the binding of the two species.

The observation of binding Gibbs free energies being close to zero with most bases suggests that two possible mechanistic scenarios are possible: one in which the base coordinates to the Lewis acid, acting as a single entity (from now on named bound pathway), and another in which they act separately (unbound pathway) with the base acting as a Brønsted base (Fig. 2). To gain further insight into the catalyst's mode of action, both pathways were explored using small molecule model compounds. Methyl benzoate was chosen to mimic the polymer substrate, along with ethanol, as a mimic for ethylene glycol. $Zn(OAc)_2$/Im was chosen as the benchmark dual catalyst. For both envisaged pathways, a conformational search for intermediates and transition states (TSs) was carried out using CREST, version 2.12[41,42] with GFN2-xTB,[43] followed by DFT optimisation and single point energy calculations, and final computation of the quasi-harmonic Gibbs free energies with GoodVibes.[44] The large difference in the activation barriers showed in the energy profiles of the glycolysis of PET catalysed by $Zn(OAc)_2$/Im ($\Delta\Delta G^{\ddagger}$ = +7.9 kcal mol^{-1}, Fig. 4) suggested that the reaction is likely to follow the bound pathway, where the proton transfer occurs with one of the acetates ($\mathbf{TS_{III-IVa}}$).

The influence of the base on the catalytic mechanism was next probed by investigating the TSs of the bound and unbound pathways for catalytic systems $Zn(OAc)_2$/DMA, $Zn(OAc)_2$/ABCO and $Zn(OAc)_2$/DBU, which feature bases with a lower (5.0) and greater (11.0, 13.5) pK_aH, respectively, than that of imidazole (6.9). These TSs were modelled from the lowest energy conformers of the $Zn(OAc)_2$/Im system, by replacing Im

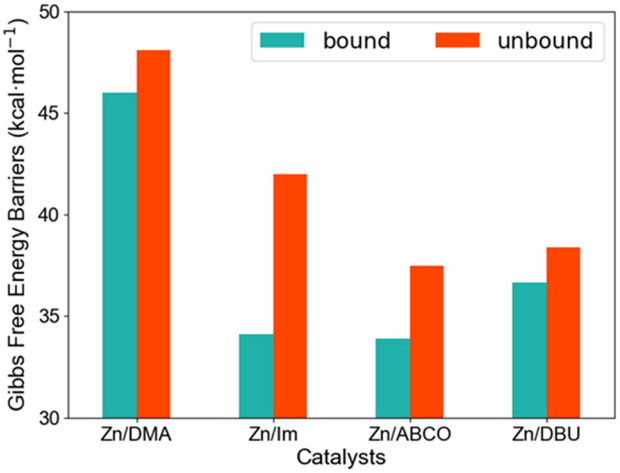

Fig. 5 Gibbs free energy barriers (bound and unbound pathways) as a function of the $Zn(OAc)_2$/base systems (base = DMA, Im, ABCO, DBU). The systems were optimised at ωB97X-D/6-31G(d) level of theory and with single point energy calculation at the ωB97X-D/def2-TZVP level of theory, both with the CPCM implicit solvent model for 1,2-ethanediol at 453 K (ε = 19.1).[45]

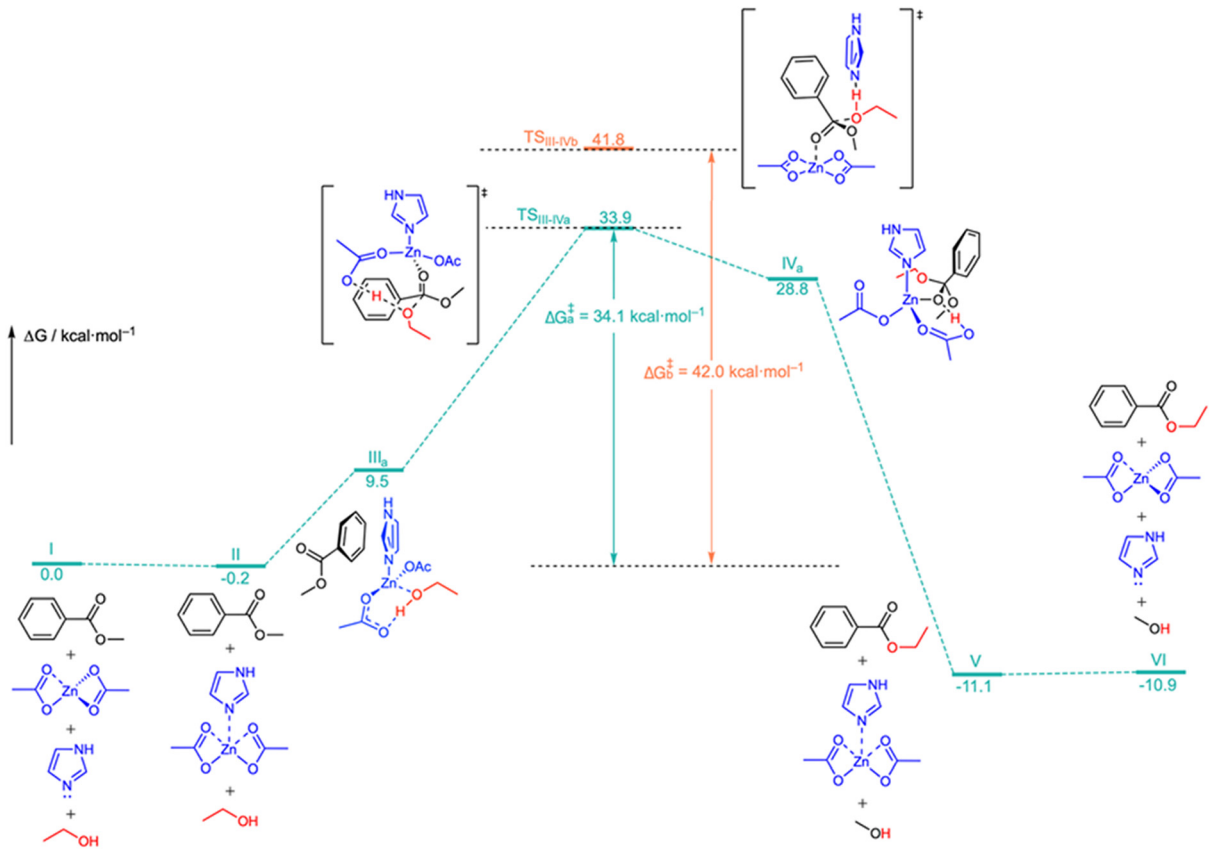

Fig. 4 PET glycolysis catalysed by $Zn(OAc)_2$/Im in the bound (green) and unbound (orange) pathways: calculated Gibbs free energy profile at 453.15 K. The structures were optimised at ωB97X-D/6-31G(d) level of theory and with single point energy calculation at the ωB97X-D/def2-TZVP level of theory, both with the CPCM implicit solvent model for 1,2-ethanediol at 453 K (ε = 19.1).[45]

with DMA, ABCO and DBU (see SI). After DFT optimisations and single point energy calculations, the Gibbs free energy barriers for the two pathways were plotted for each dual catalyst (Fig. 5).

Although no correlation was found between the energy barriers and the pK_aH of the base or the $\Delta G_{binding}$ of the dual catalysts, the bound pathway is favoured over the unbound pathway for the four bases. Furthermore, $Zn(OAc)_2$/Im presents a comparable barrier to that of $Zn(OAc)_2$/ABCO (34.1 and 33.9 kcal mol^{-1}, respectively) despite the higher activity of the former, while the bound pathway for $Zn(OAc)_2$/DBU presents a higher barrier than $Zn(OAc)_2$/Im. At the experimental temperature of 453.15 K, the differences in the kinetics observed result in differences of Gibbs free energies of the order of 0.1 kcal mol^{-1}, which DFT is unable to reproduce. For this reason, an explanation for the faster PET glycolysis rate promoted by $Zn(OAc)_2$/Im cannot be provided at this stage.

The DFT data collected subsequently allowed us to formulate a plausible reaction mechanism. In the first step, the zinc ion adopts a square pyramidal geometry, with imidazole coordinated in axial position, and both acetate ligands coordinated in a η^3 fashion and bidentate (Fig. 4, **II**). This is followed by the zinc ion returning to a tetrahedral geometry upon coordination of the ethanol, with one of the two now monodentate η^1 acetate ligands, activating ethanol by hydrogen-bonding, while some π–π stacking happens between the imidazole and the PET model (**IIIa**, Fig. S23). In the transition state ($\mathbf{TS_{III–IVa}}$), the carbonyl oxygen of the PET coordinates to the zinc ion, which maintains the tetrahedral geometry, replacing the ethanol. The ethanol is directed towards the carbonyl's electrophilic centre, attacking it as it is deprotonated by the acetate. This results in high-energy intermediate **IVa**, in which the tetrahedral carbon readily rearranges into a new carbonyl and an ethyl ester (**V** and **VI**). However, the higher-than-expected energy barriers calculated for $Zn(OAc)_2$/DMA (compared to experimental ones) suggest that this dual catalyst may follow a different depolymerisation mechanism. Future work will aim at exploring other possible mechanisms, including the involvement of ethylene glycol as a ligand in the catalyst.

Conclusions

This study aimed to shed light on the underlying mechanism of PET glycolysis, focusing on the activity–property relationships within dual Lewis acid/organobase catalyst systems. The findings highlight a clear correlation between the electronegativity of metal acetates and the pK_aH of the organobases, providing a predictive framework for identifying highly active catalyst combinations. Preliminary DFT calculations supported a mechanistic model in which the organobase coordinates to the Lewis acid, forming a cooperative catalytic entity, while the acetate ligand facilitates proton transfer during the reaction. While a universally applicable predictive model remains challenging, this work establishes meaningful structure–activity relationships that offer valuable guidance in selecting and optimising dual catalysts for efficient PET depolymerisation.

Author contributions

Conceptualisation: APD; methodology: APD, MJP, ABH, ABuchard; investigation: MJP, YW, ABH; supervision: APD, ABuchard, MNG; writing original draft: MJP, ABrandolese, ABH; writing review & editing: ABrandolese, APD, ABuchard, MNG.

Conflicts of interest

There are no conflicts to declare.

Data availability

The datasets supporting this article have been uploaded as part of the supplementary information (SI).

Supplementary information: detailed experimental procedures and additional characterisation data; DFT calculation details, data and associated digital repository. See DOI: https://doi.org/10.1039/d5cy01499a.

Acknowledgements

This work was supported by a University of Birmingham, Global Challenges PhD Scholarship (MJP), EPSRC (grant number: EP/X039234/1; EP/X039129/1 and EP/X039129/2, to support A. Brandolese, YW and ABH) and the Royal Society (UF/160021 and URF\R\221027 fellowship to A. Buchard). The authors gratefully acknowledge the University of Bath's Research Computing Group (https://doi.org/10.15125/b6cd-s854) for their support in this work. The Viking cluster was used during this project, which is a high performance compute facility provided by the University of York. We are grateful for computational support from the University of York, IT Services and the Research IT team.

Notes and references

1 L. Lebreton and A. Andrady, Future scenarios of global plastic waste generation and disposal, *Palgrave Commun.*, 2019, **5**(1), 1–11.
2 P. Europe, Plastics–the facts 2020, *PlasticEurope*, 2020, **1**, 1–64.
3 A. J. Martín, C. Mondelli, S. D. Jaydev and J. Perez-Ramirez, Catalytic processing of plastic waste on the rise, *Chem*, 2021, **7**(6), 1487–1533.
4 J. Payne and M. D. Jones, The chemical recycling of polyesters for a circular plastics economy: challenges and emerging opportunities, *ChemSusChem*, 2021, **14**(19), 4041–4070.
5 B. Baran, Plastic waste as a challenge for sustainable development and circularity in the European Union, *Ekon. Prawo*, 2020, **19**(1), 7–20.
6 I. Vollmer, M. J. Jenks, M. C. Roelands, R. J. White, T. Van Harmelen, P. De Wild, G. P. van Der Laan, F. Meirer, J. T.

Keurentjes and B. M. Weckhuysen, Beyond mechanical recycling: giving new life to plastic waste, *Angew. Chem., Int. Ed.*, 2020, **59**(36), 15402–15423.

7 N. A. Tarazona, R. Machatschek, J. Balcucho, J. L. Castro-Mayorga, J. F. Saldarriaga and A. Lendlein, Opportunities and challenges for integrating the development of sustainable polymer materials within an international circular (bio) economy concept, *MRS Energy Sustain.*, 2022, **9**(1), 28–34.

8 E. Feghali and T. Cantat, Room temperature organocatalyzed reductive depolymerization of waste polyethers, polyesters, and polycarbonates, *ChemSusChem*, 2015, **8**(6), 980–984.

9 L. Monsigny, J.-C. Berthet and T. Cantat, Depolymerization of waste plastics to monomers and chemicals using a hydrosilylation strategy facilitated by Brookhart's iridium (III) catalyst, *ACS Sustainable Chem. Eng.*, 2018, **6**(8), 10481–10488.

10 B. F. Nunes, M. C. Oliveira and A. C. Fernandes, Dioxomolybdenum complex as an efficient and cheap catalyst for the reductive depolymerization of plastic waste into value-added compounds and fuels, *Green Chem.*, 2020, **22**(8), 2419–2425.

11 S. Westhues, J. Idel and J. Klankermayer, Molecular catalyst systems as key enablers for tailored polyesters and polycarbonate recycling concepts, *Sci. Adv.*, 2018, **4**(8), eaat9669.

12 J. W. Chen and L. W. Chen, The glycolysis of poly (ethylene terephthalate), *J. Appl. Polym. Sci.*, 1999, **73**(1), 35–40.

13 C. Jehanno, I. Flores, A. P. Dove, A. J. Müller, F. Ruipérez and H. Sardon, Organocatalysed depolymerisation of PET in a fully sustainable cycle using thermally stable protic ionic salt, *Green Chem.*, 2018, **20**(6), 1205–1212.

14 K. R. Delle Chiaie, F. R. McMahon, E. J. Williams, M. J. Price and A. P. Dove, Dual-catalytic depolymerization of polyethylene terephthalate (PET), *Polym. Chem.*, 2020, **11**(8), 1450–1453.

15 A. J. Spicer, A. Brandolese and A. P. Dove, Selective and sequential catalytic chemical depolymerization and upcycling of mixed plastics, *ACS Macro Lett.*, 2024, **13**(2), 189–194.

16 C. Jehanno, J. Demarteau, D. Mantione, M. C. Arno, F. Ruipérez, J. L. Hedrick, A. P. Dove and H. Sardon, Selective chemical upcycling of mixed plastics guided by a thermally stable organocatalyst, *Angew. Chem., Int. Ed.*, 2021, **60**(12), 6710–6717.

17 A. C. Sánchez and S. R. Collinson, The selective recycling of mixed plastic waste of polylactic acid and polyethylene terephthalate by control of process conditions, *Eur. Polym. J.*, 2011, **47**(10), 1970–1976.

18 H. Kurokawa, M.-a Ohshima, K. Sugiyama and H. Miura, Methanolysis of polyethylene terephthalate (PET) in the presence of aluminium tiisopropoxide catalyst to form dimethyl terephthalate and ethylene glycol, *Polym. Degrad. Stab.*, 2003, **79**(3), 529–533.

19 A. M. Al-Sabagh, F. Z. Yehia, A.-M. M. Eissa, M. E. Moustafa, G. Eshaq, A.-R. M. Rabie and A. E. ElMetwally, Glycolysis of poly(ethylene terephthalate) catalyzed by the Lewis base ionic liquid [Bmim][OAc], *Ind. Eng. Chem. Res.*, 2014, **53**(48), 18443–18451.

20 F. Ahmadnian, F. Velasquez and K. H. Reichert, Screening of Different Titanium (IV) Catalysts in the Synthesis of Poly(ethylene terephthalate), *Macromol. React. Eng.*, 2008, **2**(6), 513–521.

21 C. H. Chen, C. Y. Chen, Y. W. Lo, C. F. Mao and W. T. Liao, Studies of glycolysis of poly (ethylene terephthalate) recycled from postconsumer soft-drink bottles. I. Influences of glycolysis conditions, *J. Appl. Polym. Sci.*, 2001, **80**(7), 943–948.

22 B. Liu, W. Fu, X. Lu, Q. Zhou and S. Zhang, Lewis acid–base synergistic catalysis for polyethylene terephthalate degradation by 1, 3-Dimethylurea/$Zn(OAc)_2$ deep eutectic solvent, *ACS Sustainable Chem. Eng.*, 2018, **7**(3), 3292–3300.

23 I. Olazabal, E. J. Luna Barrios, S. De Meester, C. Jehanno and H. Sardon, Overcoming the limitations of organocatalyzed glycolysis of poly(ethylene terephthalate) to facilitate the recycling of complex waste under mild conditions, *ACS Appl. Polym. Mater.*, 2024, **6**(7), 4226–4232.

24 Z. Guo, J. Wu and J. Wang, Chemical degradation and recycling of polyethylene terephthalate (PET): a review, *RSC Sustainability*, 2025, **3**(5), 2111–2133.

25 M. Babaei, M. Jalilian and K. Shahbaz, Chemical recycling of Polyethylene terephthalate: A mini-review, *J. Environ. Chem. Eng.*, 2024, **12**(3), 112507.

26 S. C. Kosloski-Oh, Z. A. Wood, Y. Manjarrez, J. P. de Los Rios and M. E. Fieser, Catalytic methods for chemical recycling or upcycling of commercial polymers, *Mater. Horiz.*, 2021, **8**(4), 1084–1129.

27 R. López-Fonseca, I. Duque-Ingunza, B. De Rivas, S. Arnaiz and J. I. Gutierrez-Ortiz, Chemical recycling of post-consumer PET wastes by glycolysis in the presence of metal salts, *Polym. Degrad. Stab.*, 2010, **95**(6), 1022–1028.

28 S. Kaiho, A. A. R. Hmayed, K. R. Delle Chiaie, J. C. Worch and A. P. Dove, Designing thermally stable organocatalysts for poly (ethylene terephthalate) synthesis: Toward a one-pot, closed-loop chemical recycling system for PET, *Macromol.*, 2022, **55**(23), 10628–10639.

29 L. Pedrini, C. Zappelli and S. J. Connon, Ionic Liquid Catalysts for Poly(ethylene terephthalate) Glycolysis: Use of Structure Activity Relationships to Combine Activity with Biodegradability, *ACS Sustainable Chem. Eng.*, 2025, **13**(4), 1424–1430.

30 H. Wang, Y. Liu, Z. Li, X. Zhang, S. Zhang and Y. Zhang, Glycolysis of poly (ethylene terephthalate) catalyzed by ionic liquids, *Eur. Polym. J.*, 2009, **45**(5), 1535–1544.

31 S. Marullo, C. Rizzo, N. T. Dintcheva and F. D'Anna, Amino acid-based cholinium ionic liquids as sustainable catalysts for PET depolymerization, *ACS Sustainable Chem. Eng.*, 2021, **9**(45), 15157–15165.

32 A. Basterretxea, C. Jehanno, D. Mecerreyes and H. Sardon, Dual organocatalysts based on ionic mixtures of acids and bases: a step toward high temperature polymerizations, *ACS Macro Lett.*, 2019, **8**(8), 1055–1062.

33 Z. Shao and H. Zhang, Combining transition metal catalysis and organocatalysis: a broad new concept for catalysis, *Chem. Soc. Rev.*, 2009, **38**(9), 2745–2755.
34 L. Deng, R. Li, Y. Chen, J. Wang and H. Song, New effective catalysts for glycolysis of polyethylene terephthalate waste: Tropine and tropine-zinc acetate complex, *J. Mol. Liq.*, 2021, **334**, 116419.
35 P. Wang, J. Liang, T. Yin and J. Yang, Simple Lewis pairs of zinc salts and organobases as bifunctional catalysts for controlled ring-opening polymerization of O-carboxyanhydrides, *Polym. Chem.*, 2019, **10**(40), 5498–5506.
36 C. Qu, X. Han, H. Wang, R. Wang, Y. Zhang, W. Sun, Z. Shi, Y. Wang and P. Yin, Synergistic Catalysis Driven by Solvent Effect: Efficient Glycolysis of Polyethylene Terephthalate (PET) by the $Zn(OAc)_2$/DBU-DMSO System, *ACS Sustainable Chem. Eng.*, 2025, **13**(31), 12496–12508.
37 S. Baliga and W. T. Wong, Depolymerization of poly(ethylene terephthalate) recycled from post-consumer soft-drink bottles, *J. Polym. Sci., Part A: Polym. Chem.*, 1989, **27**(6), 2071–2082.
38 C. H. Chen, Study of glycolysis of poly(ethylene terephthalate) recycled from postconsumer soft-drink bottles. III. Further investigation, *J. Appl. Polym. Sci.*, 2003, **87**(12), 2004–2010.
39 M. J. Frisch, G. W. Trucks, H. B. Schlegel, G. E. Scuseria, M. A. Robb, J. R. Cheeseman, G. Scalmani, V. Barone, G. A. Petersson, H. Nakatsuji, X. Li, M. Caricato, A. V. Marenich, J. Bloino, B. G. Janesko, R. Gomperts, B. Mennucci, H. P. Hratchian, J. V. Ortiz, A. F. Izmaylov, J. L. Sonnenberg, D. Williams-Young, F. Ding, F. Lipparini, F. Egidi, J. Goings, B. Peng, A. Petrone, T. Henderson, D. Ranasinghe, V. G. Zakrzewski, J. Gao, N. Rega, G. Zheng, W. Liang, M. Hada, M. Ehara, K. Toyota, R. Fukuda, J. Hasegawa, M. Ishida, T. Nakajima, Y. Honda, O. Kitao, H. Nakai, T. Vreven, K. Throssell, J. A. Montgomery Jr., J. E. Peralta, F. Ogliaro, M. J. Bearpark, J. J. Heyd, E. N. Brothers, K. N. Kudin, V. N. Staroverov, T. A. Keith, R. Kobayashi, J. Normand, K. Raghavachari, A. P. Rendell, J. C. Burant, S. S. Iyengar, J. Tomasi, M. Cossi, J. M. Millam, M. Klene, C. Adamo, R. Cammi, J. W. Ochterski, R. L. Martin, K. Morokuma, O. Farkas, J. B. Foresman and D. J. Fox, *Gaussian 16 Rev. C.01*, Gaussian, Inc., Wallingford CT, 2016.
40 M. J. Frisch, G. W. Trucks, H. B. Schlegel, G. E. Scuseria, M. A. Robb, J. R. Cheeseman, G. Scalmani, V. Barone, G. A. Petersson, H. Nakatsuji, X. Li, M. Caricato, A. V. Marenich, J. Bloino, B. G. Janesko, R. Gomperts, B. Mennucci, H. P. Hratchian, J. V. Ortiz, A. F. Izmaylov, J. L. Sonnenberg, D. Williams-Young, F. Ding, F. Lipparini, F. Egidi, J. Goings, B. Peng, A. Petrone, T. Henderson, D. Ranasinghe, V. G. Zakrzewski, J. Gao, N. Rega, G. Zheng, W. Liang, M. Hada, M. Ehara, K. Toyota, R. Fukuda, J. Hasegawa, M. Ishida, T. Nakajima, Y. Honda, O. Kitao, H. Nakai, T. Vreven, K. Throssell, J. A. Montgomery Jr., J. E. Peralta, F. Ogliaro, M. J. Bearpark, J. J. Heyd, E. N. Brothers, K. N. Kudin, V. N. Staroverov, T. A. Keith, R. Kobayashi, J. Normand, K. Raghavachari, A. P. Rendell, J. C. Burant, S. S. Iyengar, J. Tomasi, M. Cossi, J. M. Millam, M. Klene, C. Adamo, R. Cammi, J. W. Ochterski, R. L. Martin, K. Morokuma, O. Farkas, J. B. Foresman and D. J. Fox, *Gaussian 16 Rev. C.02*, Gaussian, Inc., Wallingford CT, 2016.
41 S. Grimme, Exploration of Chemical Compound, Conformer, and Reaction Space with Meta-Dynamics Simulations Based on Tight-Binding Quantum Chemical Calculations, *J. Chem. Theory Comput.*, 2019, **15**(5), 2847–2862.
42 P. Pracht, F. Bohle and S. Grimme, Automated exploration of the low-energy chemical space with fast quantum chemical methods, *Phys. Chem. Chem. Phys.*, 2020, **22**(14), 7169–7192.
43 C. Bannwarth, S. Ehlert and S. Grimme, GFN2-xTB—An Accurate and Broadly Parametrized Self-Consistent Tight-Binding Quantum Chemical Method with Multipole Electrostatics and Density-Dependent Dispersion Contributions, *J. Chem. Theory Comput.*, 2019, **15**(3), 1652–1671.
44 G. Luchini, J. V. Alegre-Requena, I. Funes-Ardoiz and R. S. Paton, GoodVibes: automated thermochemistry for heterogeneous computational chemistry data, *F1000Research*, 2020, **9**, 291.
45 H. W. Horn, G. O. Jones, D. S. Wei, K. Fukushima, J. M. Lecuyer, D. J. Coady, J. L. Hedrick and J. E. Rice, Mechanisms of Organocatalytic Amidation and Trans-Esterification of Aromatic Esters As a Model for the Depolymerization of Poly(ethylene) Terephthalate, *J. Phys. Chem. A*, 2012, **116**(51), 12389–12398.
46 C. Y. Legault, *CYLview, 1.0b*, Université de Sherbrooke, 2009, http://www.cylview.org.

